UNITED STATES DEPARTMENT OF THE INTERIOR

GEOLOGICAL SURVEY

MEASUREMENT OF THE REMANENT MAGNETIZATION OF IGNEOUS ROCKS

By

Richard R. Doell and Allan Cox

Open-file report 708

1964

CONTENTS

ILLUSTRATIONS

TABLE

MEASUREMENT OF THE REMANENT MAGNETIZATION OF IGNEOUS ROCKS

By Richard R. Doell and Allan Cox

ABSTRACT

The design of a simple motor-driven spinner magnetometer for measuring remanent magnetization in the range 1×10^{-5} to 1.0 emu/cc is presented, including practical details of mechanical components and electronic circuits, and procedures of operation and calibration. In routine use over a two-year period, two of these instruments have measured directions of remanent magnetization of rock specimens with an estimated accuracy of 1° and intensities with an estimated accuracy of several percent; they have required infrequent calibration and only minor maintenance. Computational techniques are given for calculating magnetic moments and directions from magnetometer output data using either graphical procedures or numerical methods suitable for machine calculation. The design of a light-weight portable drill for coring samples *in situ* and procedures for accurately orienting cores using a mechanical stage are also given.

INTRODUCTION

Most igneous rocks have natural remanent magnetizations in the range 10^{-4} to 10^{-2} emu/cc, although intensities as high as several emu/cc may be encountered near areas where lightning bolts have struck (Cox, 1961; Graham, 1961). For paleomagnetic research on igneous rocks, an instrument with a sensitivity somewhat greater than 10^{-4} emu/cc is generally needed in order to measure the remanent magnetization of rock specimens after they have been partially demagnetized. This report describes a spinner type magnetometer

suitable for magnetic analysis of most igneous rocks. It is capable of accurately measuring remanent magnetizations in the range 1×10^{-5} to 1.0 emu/cc with an ultimate sensitivity of 10^{-6} emu/cc. Long-term stability, measurement accuracy, and efficiency of operation, rather than high sensitivity were primary considerations in the design of this instrument, which is a variation of instruments previously described by Johnson and McNish (1938) and Nagata (1961, p. 58-64).

Acknowledgments

We wish to thank Mr. M. Lillard for construction of the spinner magnetometers, field core drills, and associated equipment; we are indebted also to Messrs. T. Robinson and E. Roth for assistance with the measurements used for analyzing the operation of the spinner magnetometers.

The spinner-type remanent magnetometer

instrument description

The general arrangement of the apparatus is depicted in figure 1. A nonmagnetic shaft, rotated at 109 c.p.s. (6,540 r.p.m.) by an induction-type electric motor, is fitted with a specimen holder at one end and reference magnets at the other. The specimen and reference magents thus induce signals of the same frequency in their respective pickup coils. The signal from the reference coils passes first through a phase shifter which shifts the output phase at angles from 0° to 360° with respect to the input phase angle, and then through a voltage attenuator which varies the reference signal amplitude over a range of one to 1×10^{-6}. The output signal from the reference attenuator is added to the signal from the specimen pickup coil in a mixing circuit, and the sum is amplified, filtered, and displayed on a cathode ray oscilloscope.

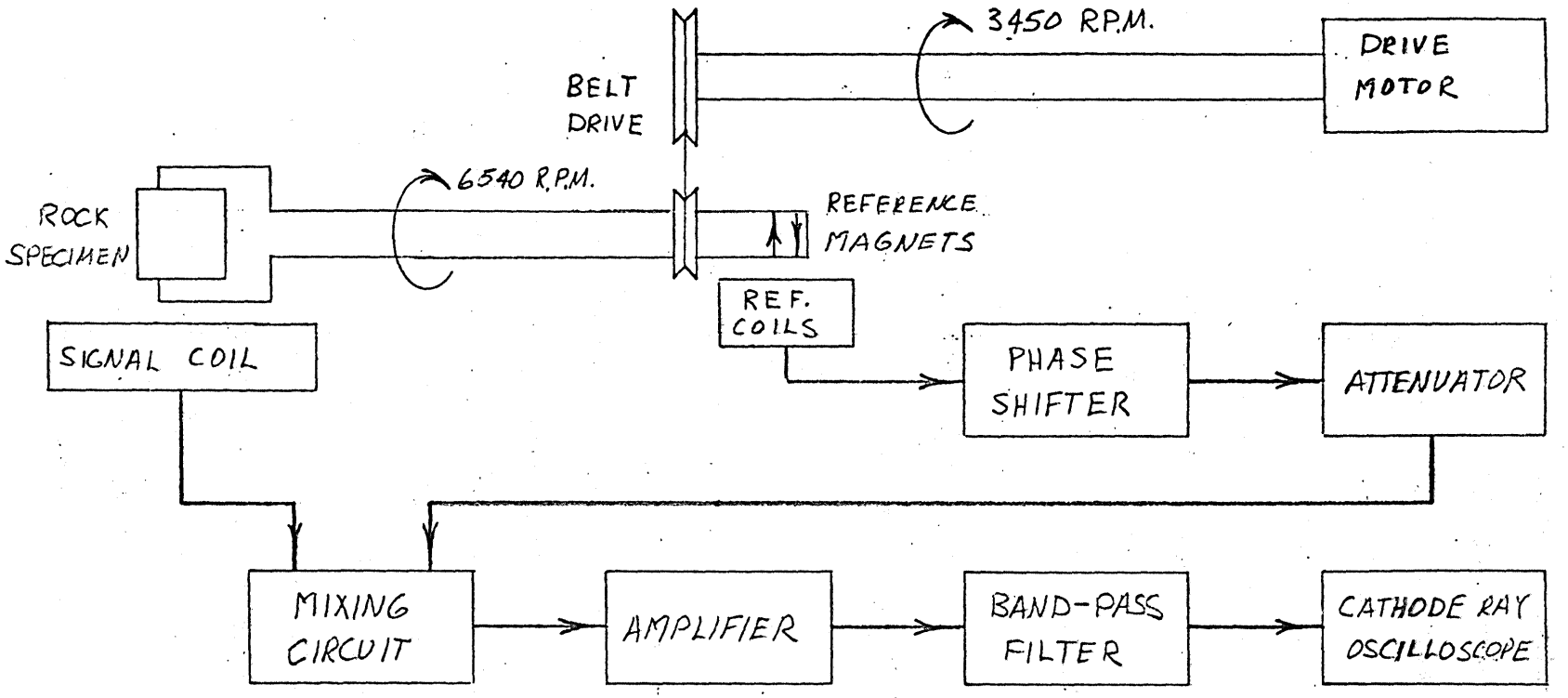

Figure 1. Block diagram of spinner-type remanent magnetometer.

The reference signal phase shifter and attenuator are so calibrated that when the two signals entering the mixing circuit sum to zero, the direction of the specimen's magnetic moment projected normal to the shaft axis is read directly from the phase shifter dial and the intensity of this moment, in electromagnetic units, is read from the attenuator dials.

Because the signal coil, reference coils, phase shifter, attenuator, and mixing circuits are all passive networks, they are not subject to electronic drift and therefore do not need repeated calibration. Changes in the electronic circuits of the amplifier, filters, and cathode ray oscilloscope affect only the ease with which null signals may be read and do not affect calibration.

Figure 2 is a photograph of the mechanical parts of the apparatus, and figure 3 shows a detailed drawing of the signal generating portion of the unit. The specimen, a cylinder 2.49 cm in diameter by 2.28 cm long, is clamped in a cubical holder of clear plastic, which in turn fits into a square indentation at one end of the shaft (fig. 8). The other end of the shaft, which is constructed from laminated phenolic material, supports two disc-shaped permanent magnets that have been magnetized in opposite directions along their diameters. The shaft rotates in two bronze bushings supported in a brass-bearing support, and is driven by a 1/3-horsepower, induction-type electric motor through a 2 meter long shaft and a V-belt drive. The motor is sufficiently powerful to operate within 1 percent of its rated speed under all normal load and power-line variations and is far enough removed from the pickup coils so as not to induce unwanted signals in the detecting units.

The specimen pickup coil is of the balanced type—that is, the outer windings are in opposition to the inner windings and are so chosen that the net flux linkage from uniform magnetic fields through the two coils is zero.

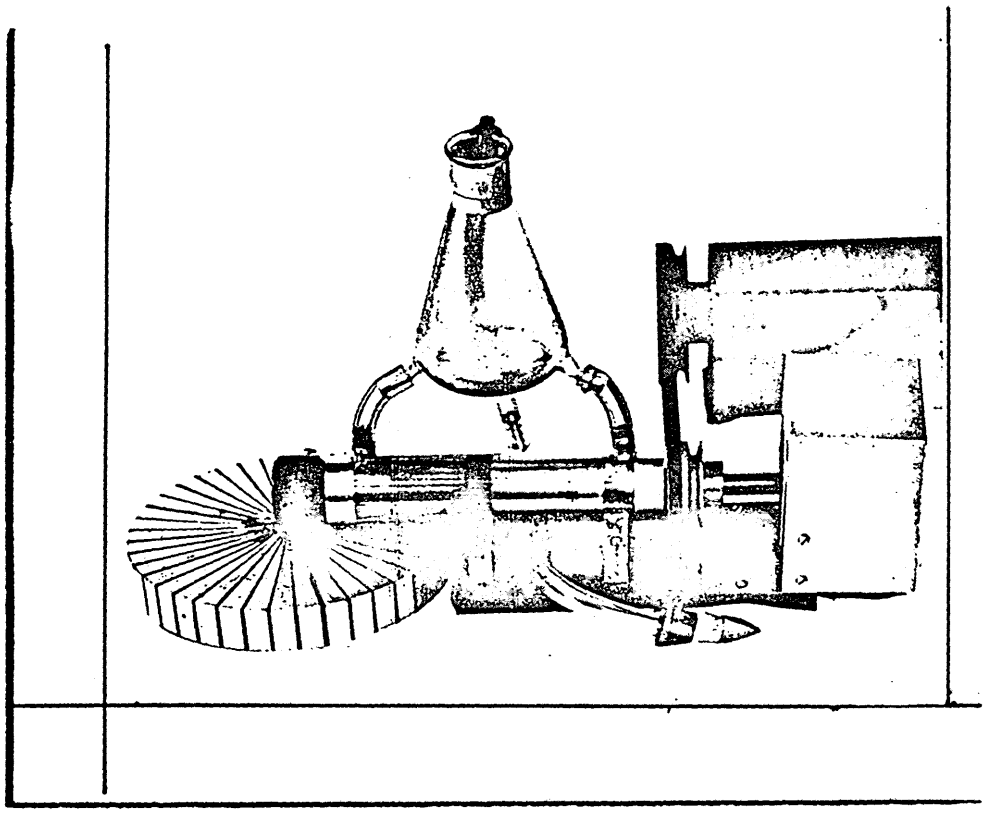

Figure 2. Mechanical portion of remanent magnetometer.

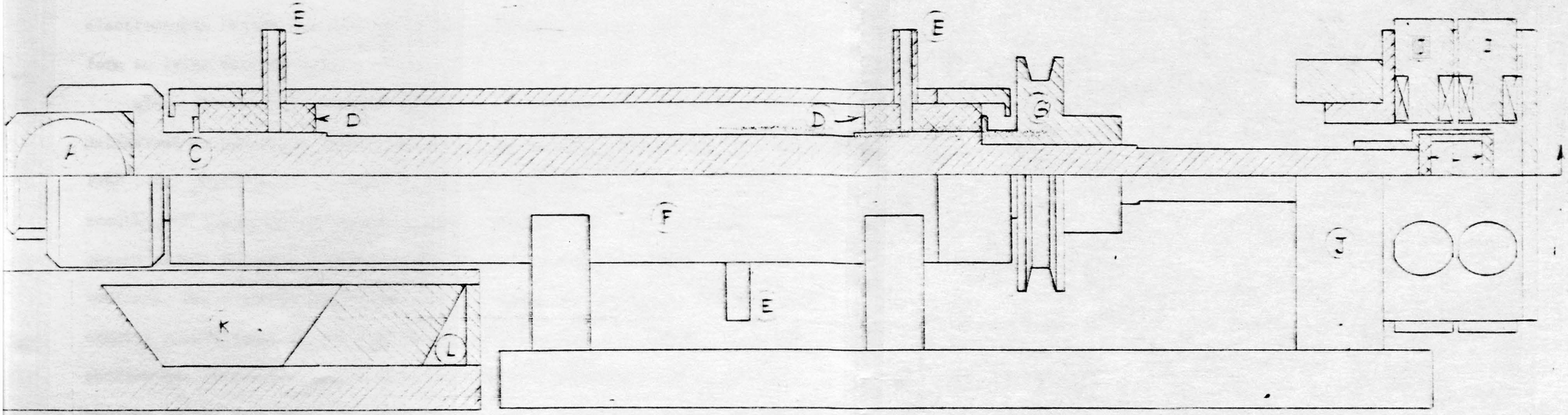

A SPECIMEN
B SPECIMEN HOLDER
C SHAFT
D SHAFT BEARINGS
E LUBRICATION FITTINGS
F BEARING SUPPORT
G DRIVE PULLEY
H REFERENCE MAGNETS
I REFERENCE COIL CORES
J REFERENCE GENERATOR SUPPORT
K MAIN PICKUP COIL
L BALANCING COIL

Figure 3. Mechanical details of specimen coil, specimen shaft, and reference signal generator.

The rationale for the shape of the windings is described on page 31. On our instrument, the inner winding contains 1,800 turns of #26 AWG copper transformer wire and the outer windings have 187 turns of #24 wire. The coil impedance at 109 c.p.s. is 87 ohms. The entire pickup coil is covered by an electrostatic shield constructed of thin aluminum strips, arranged so as to form no large current loops.

Since the unknown specimen signal in a magnetometer of this type is determined by comparison with a known reference signal (Bruckshaw and Robertson, 1948), the measurement accuracy is strictly limited by the stability and accuracy of the reference signal system. Ideally, the reference signal phase angles should be exactly equal to the angular position of the dial which indicates the magnetic direction, and the output of the attenuator should be exactly proportional to the dial which indicates magnetic moment. The phase shifter and attenuator should also function independently, and it is convenient if the reference signal is large enough to measure strong magnetic moments directly without attenuation of the signal from the specimen pickup coil.

In our instrument a large 3-phase reference signal is generated by rotating two disc-shaped magnets, 19 mm in diameter by 1.25 mm thick, near 12 stationary pickup coils. Since the magnets have rather large moments, they are aligned in opposite directions and carefully astaticized to produce no detectable signal in the specimen pickup coil (see section on alignment and calibration). The reference coils are placed at 60° intervals about the two reference magnets, and each coil contains 1,500 turns of #44 AWG copper transformer wire wound on a soft iron core. Three groups of four coils, each with the same phase angle,

are connected together in series fashion, and at 109 c.p.s. each group has an impedance of about 280 ohms. The position of each coil can be adjusted radially in order to balance the 3-phase signal during the alignment and calibration procedure.

The phase shifter, attenuator, and mixing circuits, shown schematically in figure 4 are all placed in a single cabinet (fig. 5). The phase shifter is a commercial electromechanical unit commonly used in servo-system applications. Its three stationary primary windings have impedances of about 300 ohms, and the secondary winding, a rotating armature, has an impedance of 500 ohms. When the primary windings are supplied with the 3-phase signal from the reference signal generator, the output of the secondary armature has a constant amplitude and a phase angle that varies directly with its angular position. The armature is fitted with a dial scribed from 0° to 360°.

The attenuator consists of ganged 10-turn potentiometers R2 (500 ohms) and R3 (300 ohms) designed to vary linearly the voltage appearing across R5 (550 ohms) by a factor of one to one-tenth. They are fitted with a three-digit dial. The unit labeled "decade attenuator" is a commercial "T" type voltage attenuator (600 ohm impedance) that may be set for 0 to 100 db attenuation in 20 db steps. Thus, voltages from the full value to 1×10^{-6} of the full value may be obtained at the output of the decade attenuator, and are adjustable to 1 percent of the output value. R4 (5K ohms) is a calibrating resistor (see section on calibration) and the switch S1 allows either the specimen coil signal or the attenuator output signal to be observed independently. These two signals are mixed under normal operation in the primary of transformer T1 and the secondary is connected to the

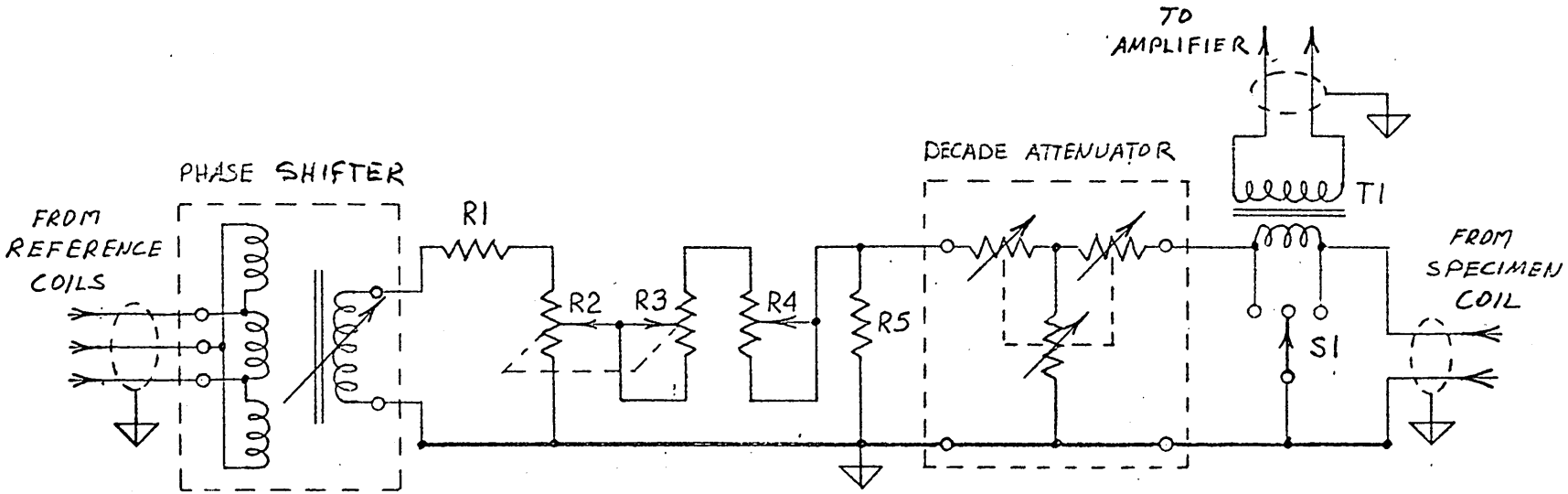

Figure 4. Schematic diagram of phase shifter, attenuator, and mixing circuits.

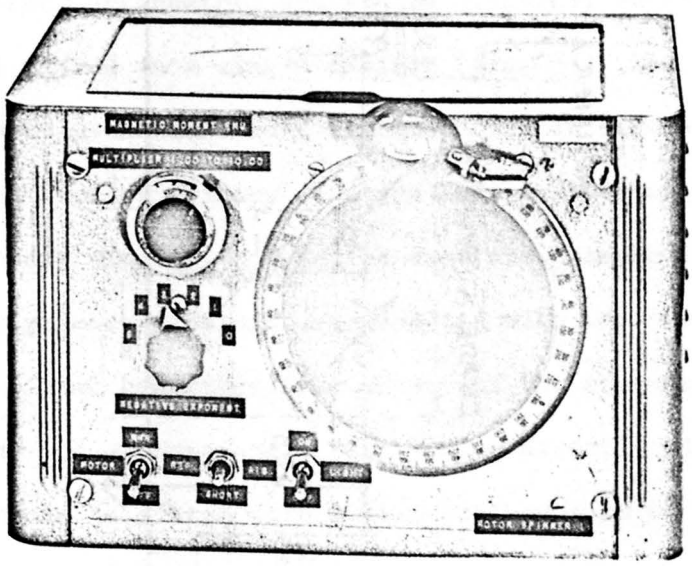

Figure 5. Phase shifter, attenuator, and mixing circuit chassis.

voltage amplifier. T1 has a primary impedance of 125 ohms, a secondary impedance of 39,000 ohms, and a turns ratio of 1:18. Resistor R1 has a value of 22 ohms.

The amplifier is a commercial unit with low input noise level and adjustable gain from 0 to 85 db. Its input impedance is about one megohm and the output impedance is 3,000 ohms. A schematic of the band pass filters, which are of the electronic feedback type (Gray, 1954, p. 682-685), is shown in figure 6. The ganged potentiometers R5-R9 and R6-R10 adjust the band-pass center frequency (coarse and fine adjustment, respectively), and the resistors R13 (fine) and R14 (coarse) adjust the width of the pass band and the Q of the filter frequency response. The cathode ray oscilloscope used as a null detector is a general purpose unit with moderate input sensitivity.

Alignment and calibration

To astaticize the reference magnets with respect to the specimen pick-up coil, the inner reference magnet is magnetized to saturation along a diameter and then partially demagnetized in an alternating field of 300 oersted peak value for stability. The outer magnet is magnetized to saturation in the opposite sense and then partially demagnetized in steps until no signal can be observed at the highest sensitivity level of the null-detector system, as described below.

After the calibration adjustment resistor R4 has been roughly adjusted using a known test magnet or the calibration circuit described below, the three signals from the reference coils are balanced. The most sensitive way of adjusting the reference coils is to observe the output of the phase shifter rather than to observe the intensity of the reference coils directly. A test

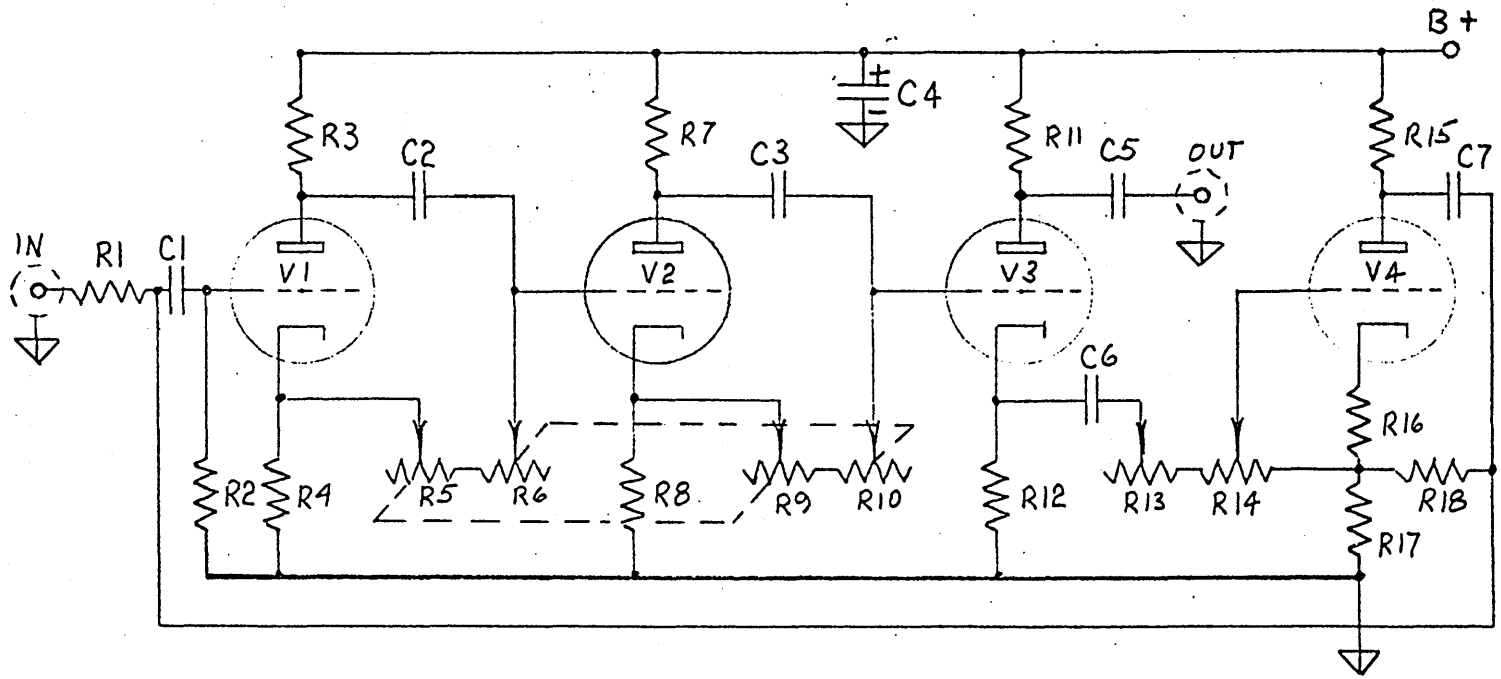

R1 = 330 K
R2 = 1 M
R3 = R4 = R16 = 1.8 K
R5 = R9 = 500 K
R6 = R10 = R13 = 50K

R7 = R8 = R17 = 3.9 K
R11 = R15 = 22 K
R12 = 5.6 K
R14 = 250 K
R18 = 470 K

C1 = C5 = C6 = C7 = .05 μ
C2 = C3 = .005 μ
C4 = 40 μ
V1 = V2 = V3 = V4 = ½ 12AX7
B+ = 135 v. REGULATED

Figure 6. Schematic diagram of band-pass filters.

magnet or rock specimen is placed in the specimen holder, measured, rotated within the holder exactly 30° about the shaft axis and remeasured; the process is repeated for 12 measurements. The phase-dial readings and attenuator settings are then plotted against the test magnet angles. Ideally the phase-dial reading should be a linear function of the test-magnet angle over the entire range 0° to 360° and the attenuator settings should be constant; by trial and error the coils are moved radially until this condition is attained. We have been able to obtain phase linearity to about 0.1° and constant amplitude to within 1 percent. After the 3-phase reference signal is balanced, the phase dial may then be placed on the shaft of the phase shifter so that it reads 0° when the test specimen has its moment aligned with the zero reference mark on the specimen holder.

The next step is to adjust exactly the intensity calibration resistor R4. The output of the attenuator is linear for all ranges except for the 0 db setting of the attenuator. Thus, if a specimen or test magnet is available with accurately known moment (less than 0.1 emu), the 20 db to 100 db attenuation ranges of the instrument may be calibrated by setting the attenuator to the known moment of the magnet and adjusting resistor R4 to give a null on the oscilloscope. For the rarely used 0 db attenuation range, a calibration chart must be prepared.

Standard magnetic specimens may be used to prepare this calibration chart and to check the linearity of the instrument. An alternative calibration method which uses an alternating current meter as a primary standard is shown in figure 7. The specimen pickup coil is replaced by an auxiliary coil and a magnet is rotated in the specimen holder. The signal induced in the auxiliary coil is amplified by a power amplifier and supplied to a test

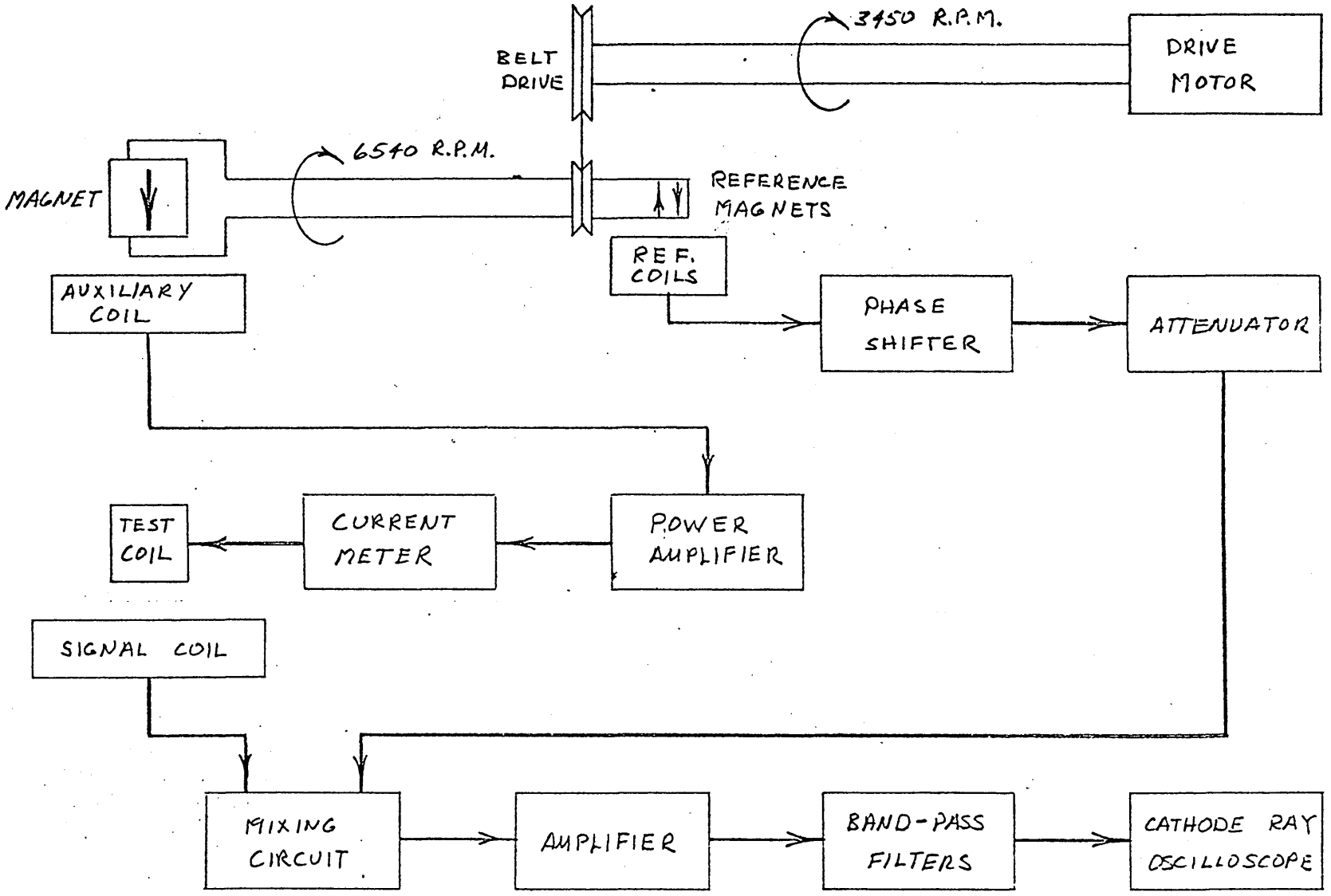

Figure 7. Block diagram of procedure for calibration of spinner magnetometer.

coil through an accurate current meter. Our test coil consists of a single layer of 39 turns of #24 AWG copper transformer wire wound on a cylindrical form, 2.49 cm in diameter by 2.28 cm long (the specimen size). During the test, its axis is aligned along the specimen pickup coil axis, and it is placed at the same distance from the pickup coil that a specimen would have during normal operation. It induces a signal in the specimen pickup coil equivalent to a specimen of magnetic moment:

$$M \text{ (e.m.u.)} = 25.53 \; i_{rms} \text{ (amperes)}$$

where i_{rms} is the root-mean-square current supplied to the test coil. Thus, signals equivalent to any desired specimen magnetic moment may be induced in the pickup coil and nulled with the reference signal in the manner used for normal operation.

Since the filters are of the feedback type, it is possible to adjust resistors R13 and R14 (fig. 6) so that the units go into a self-sustained oscillation. For optimum filtering (smallest band-pass width), R13 and R14 are adjusted so that the filters are just below the point where sustained oscillation occurs. Then with the spinner running and a signal appearing on the oscilloscope, the resistors R5-R9 and R6-R10 are adjusted to give a maximum signal on the oscilloscope. When so adjusted, the band-pass peak is at the operating frequency of the spinner. Unless the specimens being measured have magnetic moments near the minimum values measurable on these instruments, it is not necessary to use an extremely narrow pass band and adjustments need be made only a few times each week.

During several years of operation, in which two different standard specimens were measured each week to test the operation and calibration of the magnetometers, it has not been necessary to change any of the adjustments

described above or to change the adjustment of the calibration resistor. Although it is necessary occasionally to adjust the filter circuits to improve noise rejection, it should be noted that these adjustments do not affect the calibration.

MEASUREMENT PROCEDURE

Attenuator and phase-dial readings recorded by spinning about one axis of the specimen determine only the component of the magnetic moment normal to the axis of spinning. It is therefore necessary to obtain at least one more datum by spinning the specimen about a different axis in order to determine the total magnetic moment and its direction within the specimen. Several additional measurements are desirable to minimize effects of induced magnetic anisotropy and specimen inhomogeneity, and to estimate the precision of a single determination of the remanent magnetism of a specimen.

In our system for obtaining oriented samples in the form of cores, which is described in the section on collection of samples, the specimens later cut from these samples are assigned right-handed orthogonal axes $\underline{x}$, $\underline{y}$, and $\underline{z}$. The $\underline{z}$ axis is along the specimen cylinder axis, the $\underline{y}$ axis is along the specimen diameter that was horizontal in the *in situ* position, and the $\underline{x}$ axis is along the diameter normal to the $\underline{y}$ axis. When a specimen is placed in a specimen holder (fig. 8) each of the three axes is parallel to one of the cube edges of the holder. The square indentation in the spinner shaft is arranged so that one of the axes of the specimen is in the "zero" position; this direction is marked "I" on the shaft, and the direction 90° clockwise is marked "II."

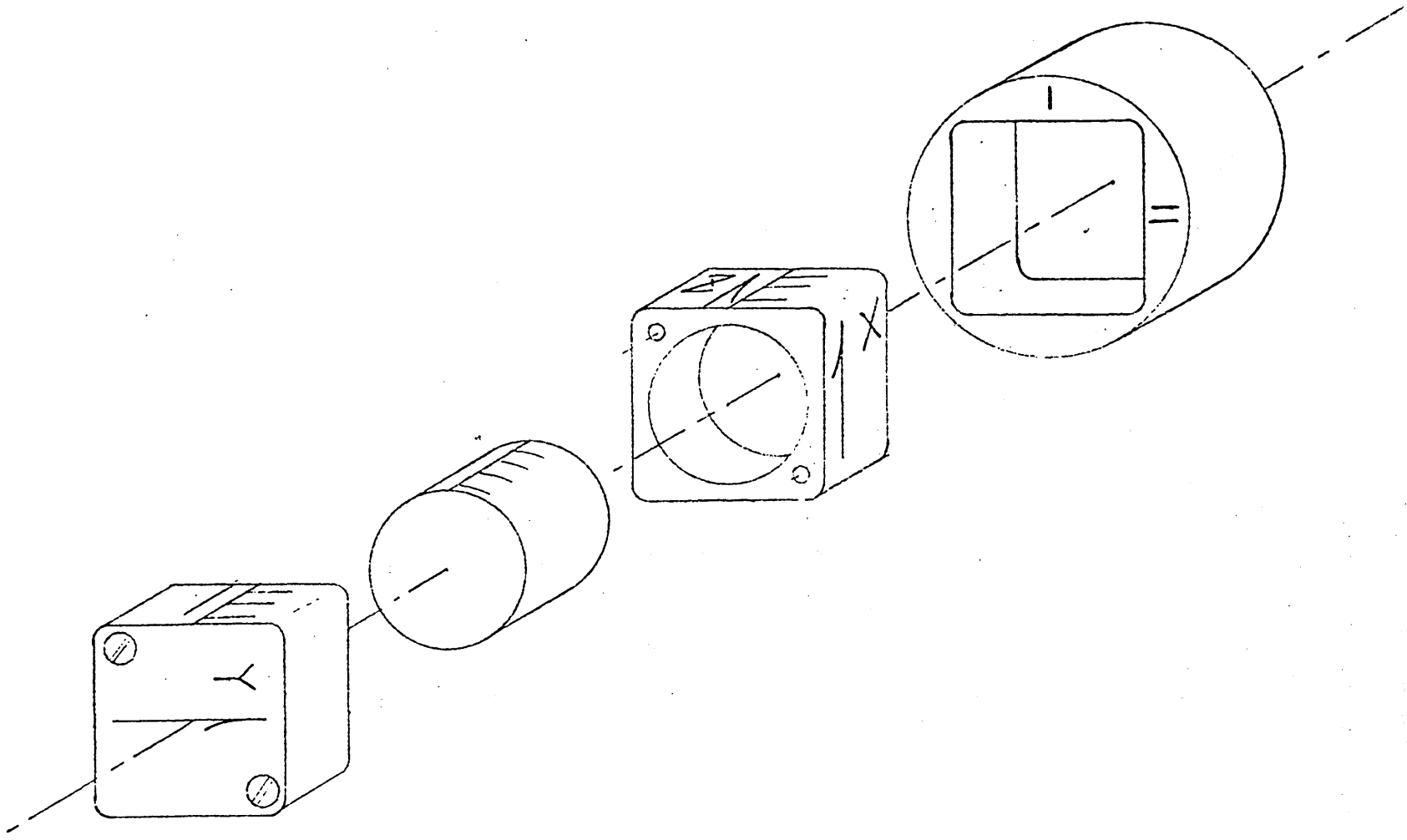

Figure 8. Rock specimen, specimen holder, and spinner shaft in position for first measurement.

After the unit is properly calibrated and the filters adjusted, a single measurement may be made as follows:

1. Place the specimen holder in the shaft in the desired position and start the shaft spinning.
2. Short out the reference signal with the switch S1 and adjust the amplifier gain so that a convenient signal from the specimen appears on the cathode ray oscilloscope.
3. Leaving the amplifier gain unchanged, move switch S1 to short out the signal from the specimen and adjust the attenuator until a signal of similar size from the reference magnets appears on the cathode ray oscilloscope.
4. Move switch S1 to its center position and alternately adjust the phase dial and attenuator until no signal appears on the cathode ray oscilloscope; as the "null" is approached, the amplifier gain should be increased so that small adjustments of the phase dial and the attenuator away from the null settings cause easily recognizable signals to appear on the cathode ray oscilloscope. The setting on the phase dial is the angle of the component of magnetization normal to the spin axis measured clockwise from the "I" mark on the shaft, and the attenuator settings record its magnetic moment in emu. Nulls usually can be easily achieved without use of the shorting switch unless intensities vary greatly between measurements.

For the complete determination of remanent magnetization of a specimen we routinely make six different signal measurements or "spins." These spins are in pairs about the three axes, so that two separate determinations of

the intensity and direction of each of the three components normal to the three axes are obtained. The component normal to the $\underline{z}$ axis is labeled $M_{\underline{z}}$, and its direction is $\phi_{\underline{z}}$, measured clockwise from the plus $\underline{x}$ direction (fig. 9). The other two components are determined by $M_{\underline{x}}$, $\phi_{\underline{x}}$, and $M_{\underline{y}}$, $\phi_{\underline{y}}$ for spins about the $\underline{x}$ and $\underline{y}$ axes, respectively.

The first or "a" spin is made with the plus $\underline{z}$ axis directed into the shaft, the plus $\underline{x}$ axis directed toward the "I" position, and the plus $\underline{y}$ axis directed toward the "II" position. The phase dial reads the angle $\phi_{\underline{z},\underline{a}}$ (see fig. 10) and the attenuator reads the magnetic moment $M_{\underline{z},\underline{a}}$. The second or "b" spin is made with the plus $\underline{z}$ axis directed out from the shaft, the plus $\underline{x}$ axis directed toward "I," and the minus $\underline{y}$ axis directed toward the "II" position. The phase-dial reading is $\phi_{\underline{z},\underline{b}}$ and the attenuator reads $M_{\underline{z},\underline{b}}$. Ideally, $M_{\underline{z},\underline{a}}$ and $M_{\underline{z},\underline{b}}$ are both equal to the true moment $M_{\underline{z}}$, $\phi_{\underline{z},\underline{a}}$ is equal to $\phi_{\underline{z}}$, and $\phi_{\underline{z},\underline{b}}$ is related to $\phi_{\underline{z}}$ by the relation:

$$\phi_z = 360° - \phi_{z,b} \tag{1}$$

These relations are shown in figure 10. Similar measurements are made by spinning about the $\underline{x}$ and $\underline{y}$ axes as summarized in table 1.

Measurements about the $\underline{z}$, $\underline{x}$, and $\underline{y}$ axes are combined in pairs as follows:

$$\begin{aligned} M_z &= \tfrac{1}{2}\left(M_{z,a} + M_{z,b}\right) \\ M_x &= \tfrac{1}{2}\left(M_{x,a} + M_{x,b}\right) \\ M_y &= \tfrac{1}{2}\left(M_{y,a} + M_{y,b}\right) \end{aligned} \tag{2a}$$

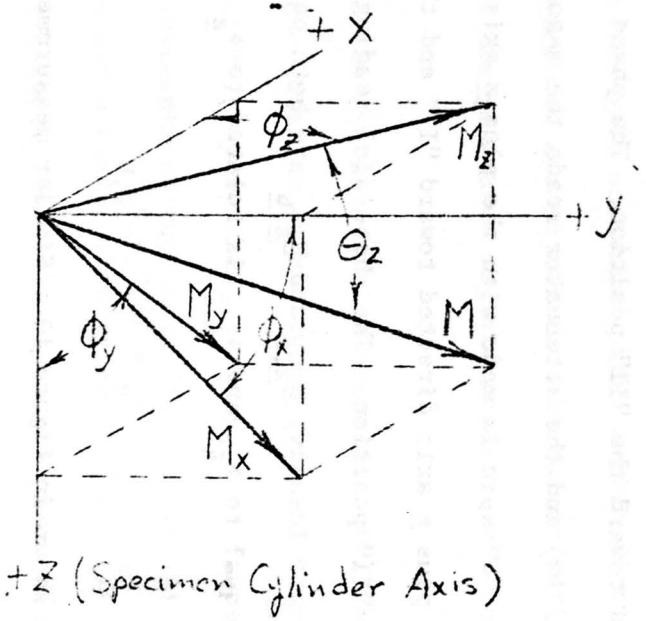

Figure 9. Designation of magnetic components within a rock specimen.

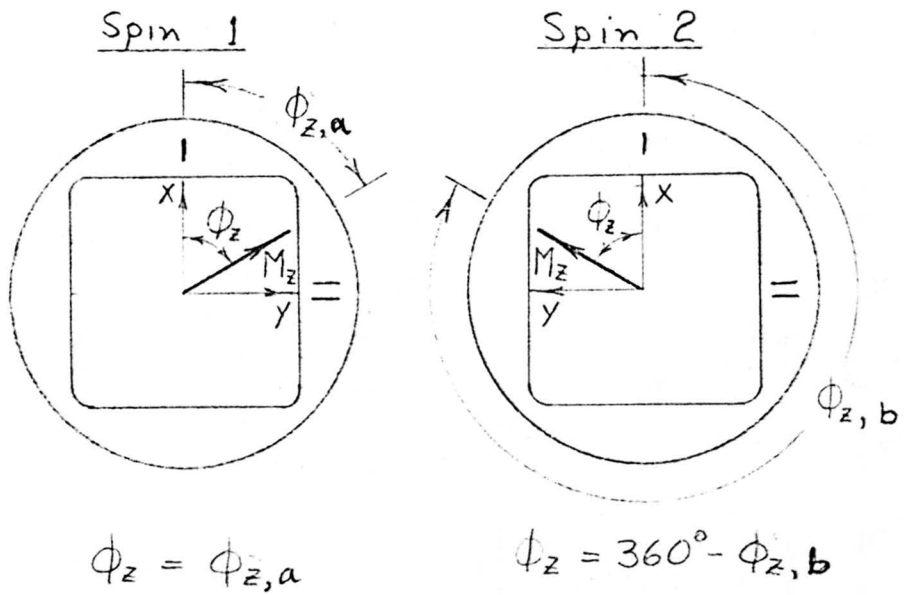

Figure 10. Angular relationships in the double-spin procedure.

Table 1.--Specimen orientations for six spins

Spin number	Axis directed into shaft	Axis towards "I" direction	Axis towards "II" direction	Data obtained	
				Moment	Angle
1	+z	+x	+y	$M_{z,a}$	$\phi_{z,a}$
2	-z	+x	-y	$M_{z,b}$	$\phi_{z,b}$
3	+x	+y	+z	$M_{x,a}$	$\phi_{x,a}$
4	-x	+y	-z	$M_{x,b}$	$\phi_{x,b}$
5	+y	+z	+x	$M_{y,a}$	$\phi_{y,a}$
6	-y	+z	-x	$M_{y,b}$	$\phi_{y,b}$

$$\phi_z = \tfrac{1}{2}\left(360° + \phi_{z,a} - \phi_{z,b}\right)$$

$$\phi_x = \tfrac{1}{2}\left(360° + \phi_{x,a} - \phi_{x,b}\right) \qquad (2b)$$

$$\phi_y = \tfrac{1}{2}\left(360° + \phi_{y,a} - \phi_{y,b}\right)$$

Use of these averages rather than a single measurement about each axis reduces possible errors due to inhomogeneity or anisotropy in the specimen, and provides redundant data to check measurement accuracy and precision. Averaging also automatically corrects for any possible systematic error in phase angle measurement, since the same error angle is added to both $\phi_{\underline{z},\underline{a}}$ and $\phi_{\underline{z},\underline{b}}$, for example, and drops out in step 2b above. When the direction of the component normal to the spin axis falls near the "I" position it is possible to have both $\phi_{\underline{z},\underline{a}}$ and $\phi_{\underline{z},\underline{b}}$, for example, fall on the same side of the zero phase reading. This may be caused by small measurement errors or by the systematic errors mentioned above. When this takes place, the expressions (2b) should be replaced by:

$$\phi_z = \tfrac{1}{2}\left(\phi_{z,a} - \phi_{z,b}\right)$$

$$\phi_x = \tfrac{1}{2}\left(\phi_{x,a} - \phi_{x,b}\right) \qquad (2c)$$

$$\phi_y = \tfrac{1}{2}\left(\phi_{y,a} - \phi_{y,b}\right)$$

The total magnetic moment is given by

$$M = \left[\left(M_z^2 + M_x^2 + M_y^2\right)/2\right]^{\frac{1}{2}} \qquad (3a)$$

$$\cong \tfrac{1}{2}\left(M_{z,a}^2 + M_{z,b}^2 + M_{x,a}^2 + M_{x,b}^2 + M_{y,a}^2 + M_{y,b}^2\right)^{\frac{1}{2}} \qquad (3b)$$

The key to finding the direction of magnetization from spinner magnetometer measurements lies in noting that during each spin the component of magnetization parallel to the rotation axis does not contribute to the signal generated in the pickup coil. Thus the angle $\phi_{\underline{z}}$ is consistent with any vector lying in a half plane having an edge along the rotation axis and extending in the direction $\phi_{\underline{z}}$, and similarly for $\phi_{\underline{x}}$ and $\phi_{\underline{y}}$. One method of determining the direction of magnetization in a specimen uses phase angles and intensities in combination. The component of the total magnetization along the $\underline{z}$ direction is given by $M_{\underline{x}} \sin\phi_{\underline{x}} = M_{\underline{y}} \cos\phi_{\underline{y}}$, and similarly for the components along the $\underline{x}$ and $\underline{y}$ directions. These pairs of values may then be averaged and the direction and intensity of magnetization in the specimen calculated from these three vector components.

An alternative method using only phase angles is preferable for most purposes because phase angles can be measured with greater precision than intensities and can easily be checked for internal consistency. As previously noted, the $\phi_{\underline{z}}$ measurement is consistent with all vectors lying in a half plane passing through the $\underline{z}$ axis, and the $\phi_{\underline{x}}$ measurement with all vectors in a plane passing through the $\underline{x}$ axis, so that the only vector consistent with both measurements is along the intersection of these two planes. The $\phi_{\underline{x}}$ and $\phi_{\underline{y}}$ measurements similarly define a unique vector consistent with both measurements, as do the $\phi_{\underline{y}}$ and $\phi_{\underline{z}}$ measurements. The mean of these three vectors may be taken as the direction of magnetization of the specimen, and the angular differences between the vectors as a measure of the precision of the measurement.

A graphical technique using an equal-area or stereographic projection has been given by Graham (1949). The planes defined by $\phi_{\underline{z}}$, $\phi_{\underline{x}}$, and $\phi_{\underline{y}}$ are drawn as great circles on the projection (fig. 11), and usually intersect to form a small error triangle. The radius of the circle inscribed in this triangle is commonly used as a relative measure of the precision of the measurement, and its center, defined by the angles $\overline{\phi}_{\underline{z}}$ and $\overline{\theta}_{\underline{z}}$, is commonly used as the best estimate of the direction of magnetization. A relatively minor difficulty in using this method for determining the mean direction arises when the magnetization of the specimen is nearly parallel to a rotation axis. Signals which are weaker and less well defined than the others are generated on spinning about that axis, but the plane defined by these weaker spins is given nearly equal weight if the center of the inscribed circle is taken as the direction of magnetization. This factor can be qualitatively considered by taking the best estimate of the magnetic direction nearer the intersection of the two planes defined by the stronger signals. A quantitative analytical method for weighting the stronger and more reliable measurements is given in the section on use of a computer to reduce spinner magnetometer data.

To find the magnetic declination $\underline{D}$ and inclination $\underline{I}$ corresponding to the original orientation of the specimen, let α be the geographic azimuth of the horizontal $\underline{y}$ axis, β the plunge of the $\underline{z}$ axis, $\overline{\phi}_{\underline{z}}$ the azimuth of the magnetic vector reckoned clockwise from $\underline{x}$ in the $\underline{xy}$ plane, and $\overline{\theta}_{\underline{z}}$ the inclination of the magnetic vector above (-) or below (+) the $\underline{xy}$ plane, as shown in figure 12. The $+\underline{z}$ axis is first rotated $(90 - \beta)$ degrees toward the $+\underline{x}$ axis, and the magnetic vector is rotated the same angular displacement along a small circle having the $\underline{y}$ axis as its center. The plane of projection thus

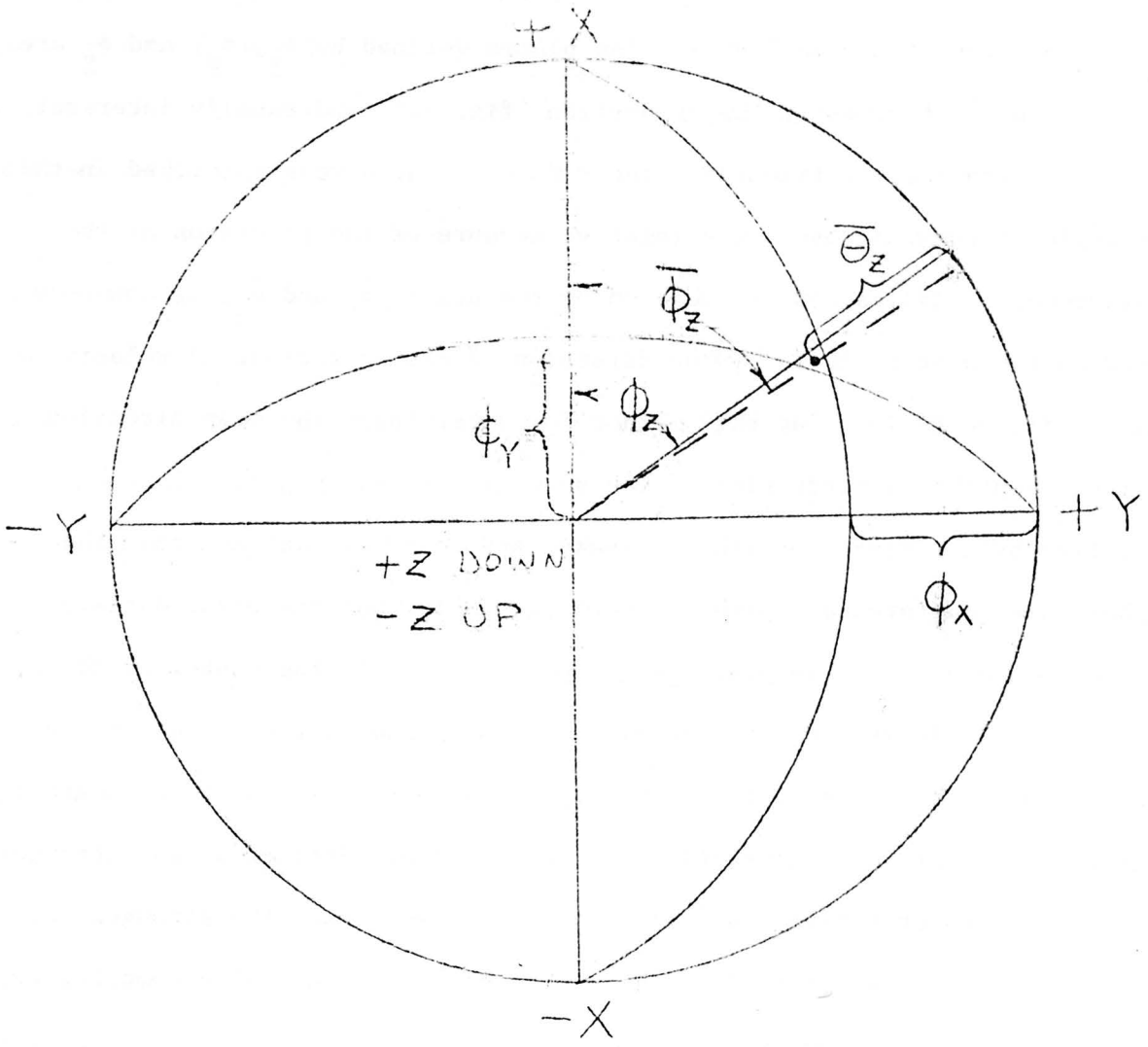

Figure 11. Graphical calculation of the direction of remanent magnetization within a specimen from spinner magnetometer data.

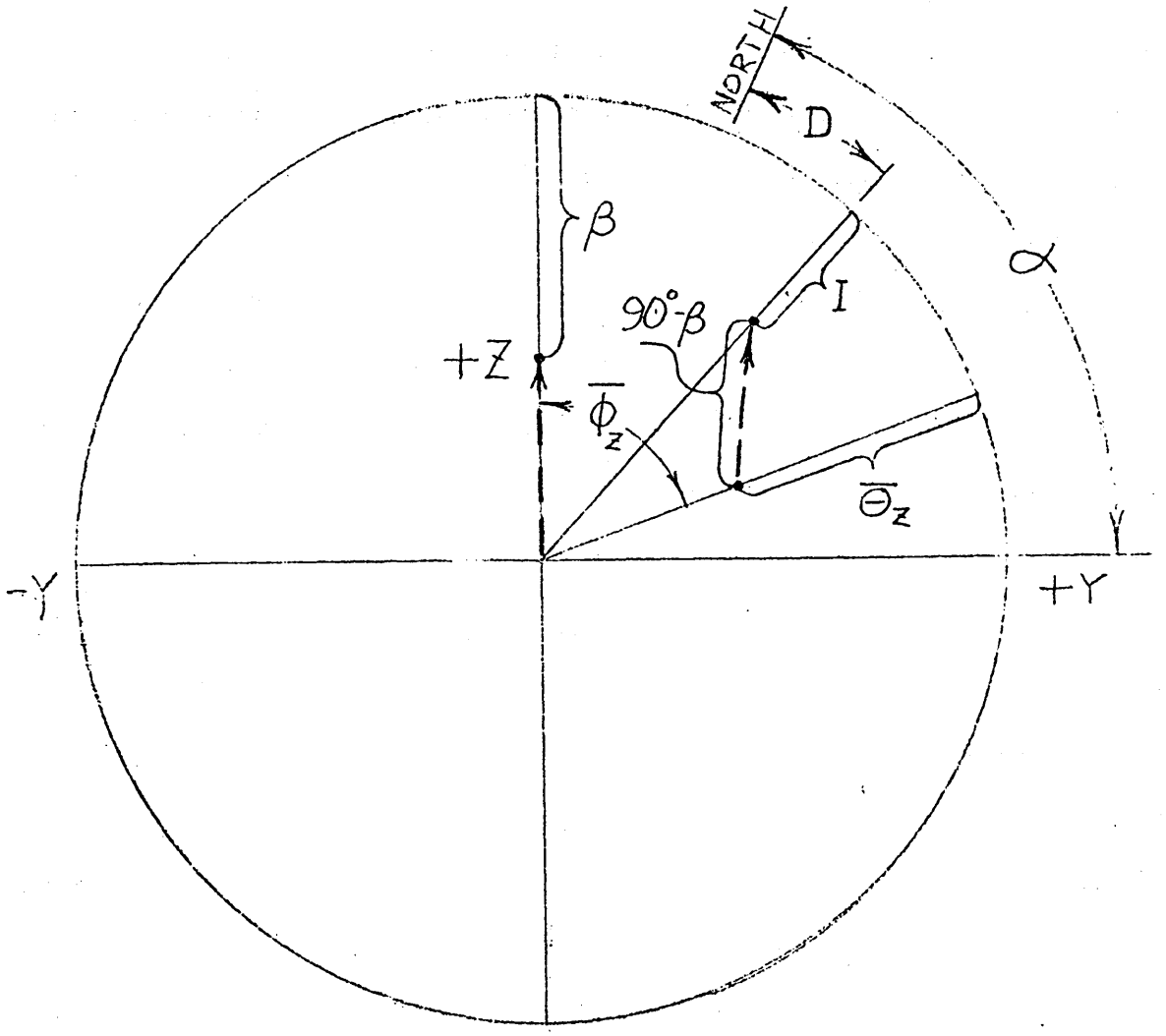

Figure 12. Graphical calculation of <u>in situ</u> direction of remanent magnetization from orientation data and specimen magnetization direction data.

becomes the horizontal plane corresponding to the original orientation of the specimen. If geographic north is marked at an angle α counterclockwise from y, then D and I may be read directly from the projection, as indicated in figure 12.

A program for carrying out all of the calculations described in this section on a digital computer, along with additional calculations designed to check the internal consistency of the phase angle and intensity measurements is given below.

PRECISION AND ACCURACY OF MEASUREMENT

Instrumental precision was determined by making nine repeated measurements on a specimen with an intensity of magnetization of 1.5×10^{-3} emu/cc. When the specimen was removed from the holder between successive measurements, the direction of magnetization could be measured with a reproducibility of 0.7° (s.d.) and the intensities to 1.1 percent (Doell and Cox, 1963). When the specimen was left in the holder between successive measurements the reproducibility was 0.2° (s.d.), indicating that measurement precision is primarily limited by the accuracy with which specimens can be aligned in the holder.

The measurement accuracy of these instruments may be conveniently separated into several parts: (1) the accuracy of the original calibration, (2) the rate of drift or change in this calibration with time, and (3) the amount of error introduced in the measurements by such factors as specimen shape, specimen inhomogeneity, and susceptibility anisotropy.

During the original alignment and calibration procedures set forth above, the reference signal system may be adjusted so that a phase angle, corresponding to a magnetic component direction, is determined to within $\pm 0.1°$.

The accuracy of the intensity determination depends on the linearity of the attenuator units, rated as 1 percent, and on the accuracy of the alternating current meter used in setting the calibration resistor R4. Our meter is rated as 1 percent.

Any change in the output signal from the reference system between calibration checks will reduce the accuracy of the measurements, and small changes are expected if the magnetic moments of the reference magnets change, if the rotation frequency changes, or if the shaft changes alignment due to bearing wear. As a routine check on instrument performance, a small bar magnet (2.1×10^{-2} emu) has been measured at weekly intervals, and these data may be used to provide an estimate of the drift. Independent measurements by two operators using two magnetometers evaluated over a one-year period showed a standard deviation of 1.8° in direction and 2.4 percent in intensity. These values are not very much larger than the precision values, and may in part be due to drift in the bar magnets rather than instrumental drift.

The accuracy of measurements may also be influenced by the shape of the specimens since for a cylindrical specimen the magnetic field sensed at the pickup coil depends not only on the direction and intensity of the remanent magnetization, but also on the orientation of the cylinder axis in the specimen holder. It should be noted that this effect is quite different from the change in magnetization of a specimen due to the internal demagnetizing field, which also depends on the shape of the specimen; the former represents the nondipolar part of the field outside the specimen due to its shape, and the latter the effects of the demagnetizing field inside the specimen. To determine the magnitude of the external shape effect on the present instrument,

each of four specimens from different lava flows was magnetized to saturation along 11 different directions in a constant magnetic field of 7,000 oe. The measured directions of these saturation remanent magnetizations differed from the known directions of the applied field by average angles of .65°, .69°, .99°, and 1.04° for the four specimens, and intensity variations were well under 1 percent. Because individual angular errors showed no systematic relationship to the directions of the applied field, they were not due to the external shape effect; they probably are due to errors in measurement and errors in aligning the specimen in the 7,000 oe magnetic field. From these and other related experiments, we conclude that the effect of specimen shape is negligible, and that the calibration procedure previously described may be used for specimens magnetized in any direction, even though the geometry of the calibration coil corresponds to a specimen magnetized along its axis.

To test the influence of specimen inhomogeneity on the accuracy of measurement, a test specimen was assembled from 10 thin cylindrical disks cut from a homogeneous basalt. The test specimen was given a saturation remanent magnetization along its axis and was then repeatedly measured after various disks had been replaced by nonmagnetic blanks. These measurements were also repeated with the same specimen magnetized to saturation along a diameter and along a direction 45° to the cylindrical axis. In all, 98 configurations were investigated, some consisting almost entirely of blanks and others almost entirely of magnetic disks. The results of these experiments may be summarized as follows. No systematic differences in direction greater than about 1° were observed, nor were there intensity

differences greater than several percent. Moreover, errors this large were observed only for the more extreme configurations. Measurement errors due to inhomogeneities commonly encountered in rock specimens thus appear to be negligible.

Anisotropy of susceptibility may also give rise to spinner magnetometer measurement errors. An analysis of this problem is beyond the scope of the present report; however, it can be shown that the double-spin procedure for measurements about each axis reduces errors of this type to a point where they are negligible for rocks commonly used in paleomagnetic research.

SPECIMEN PICKUP COIL DESIGN

The expressions and considerations developed here were used to design a spinner magnetometer specimen pickup coil that would have a maximum signal to noise ratio, given the present mechanical configuration. The coil response equations given here are expressed in differential forms so that the total response of a coil of any desired shape may be obtained by integrating the appropriate equations over the total cross-section area of the coil.

The flux linkage of an incremental cross-sectional area, $\underline{d}\ \underline{A}$, of the coil at radius $\underline{r}$ and distance $\underline{z}$ from the center of the specimen (here approximated by a magnetic dipole) (fig. 13) is:

$$d\phi = 2\pi M_i\ n\ r^2 / \left(r^2 + z^2\right)^{\frac{3}{2}}\ d\ A \qquad (4)$$

where $\underline{M_i}$ is the component of the magnetic moment of the specimen normal to the spin axis, here aligned along the coil axis, and $\underline{n}$ is the number of turns per unit cross section of the coil.

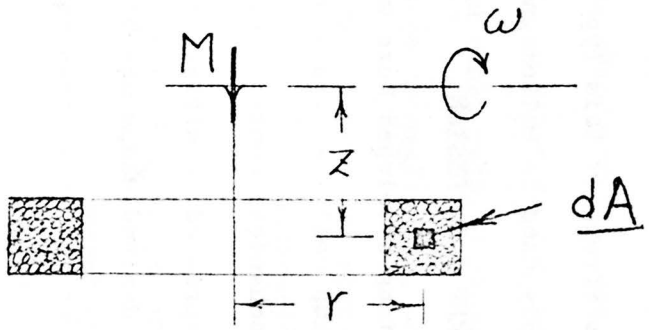

Figure 13. Relations between position of pickup coil and rotating specimen.

If n is replaced by $(\pi/4)\ (1/a)$, where a is the cross-sectional area of the wire used to wind the coil ($\pi/4$ is a winding factor), and the specimen rotates with angular frequency f, then the incremental rms voltage induced in the coil is:

$$de_s = \left(1/2\right)\left(\pi^3\ f\ M_i\right)\left(1/a\right)\left[r^2/\left(r^2 + z^2\right)^{\frac{3}{2}}\right] d\ A \qquad (5)$$

The rms thermal noise voltage of such a coil is (Gray, 1954, p. 494-499):

$$de_t = \left(4k\ T\ R\ \Delta f\right)^{\frac{1}{2}} \qquad (6)$$

where k is Boltzmann's constant, T the absolute temperature, Δf the pass-band over which de_t is measured, and R is the total resistance of the incremental cross-sectional area, $d\ A$, of the coil. Replacing R by $2\pi\ r\rho\left(n/a\right) d\ A = \left(\pi^2\ r\rho\right)/\left(2a^2\right) d\ A$, where ρ is the resistivity of the wire, (6) becomes:

$$de_t = \left(\pi/a\right)\left(2k\ T\ r\rho\ \Delta f\right)^{\frac{1}{2}} d\ A \qquad (7)$$

Another source of noise arises from voltages induced in the coil from ambient alternating fields in the laboratory. Assuming that there are no gradients in such fields over the area bounded by the coil, the rms voltage in the incremental cross-sectional area of the coil from these fields is:

$$de_f = \left(\sqrt{2}/4\right)\left(\pi^3\ f\ H_f\ r^2\right)\left(1/a\right) d\ A \qquad (8)$$

where H_f is the effective peak field strength of the component of the ambient alternating field at frequency f along the coil axis.

Forming signal to noise ratios, we find:

$$\frac{de_s}{de_t} = \frac{\pi^2 f M_i}{2\left(2kT \Delta f \rho\right)^{\frac{1}{2}}} \left[\frac{r}{r^2 + z^2}\right]^{\frac{3}{2}} \tag{9}$$

$$\frac{de_s}{de_f} = \frac{\sqrt{2}M_i}{H_f} \left[\frac{1}{r^2 + z^2}\right]^{\frac{3}{2}} \tag{10}$$

The total ratio of e_s/e_f for a coil is commonly increased by placing a larger coaxial "balancing" coil in series opposition with the main coil (with a slight reduction in e_s and e_s/e_t), or by placing the unit in a magnetic shield.

Lines of equal de_s/de_t determined from equation (9) are circles centered on the axis of rotation and passing through the center of the specimen as shown in figure 14.

These considerations and the relations (5), (9), and (10) can then be used to design an optimum coil. The important factors are:

1. The main coil should be as close to the sample as possible, with its outer cross-sectional shape bounded by a circle of equal de_s/de_t—equation (9).
2. The coil should be no larger than necessary—equation (10)—but must be large enough to yield a signal sufficient to drive the detecting units—the integral of equation (5) over the cross-section of the coil. (Note also that the overall coil size and wire cross-section area, $1/a$, will determine the coil impedance, which should be matched to the detecting unit.) Figure 14 also shows the optimum shape of a detecting coil for the spinner magnetometer described above.

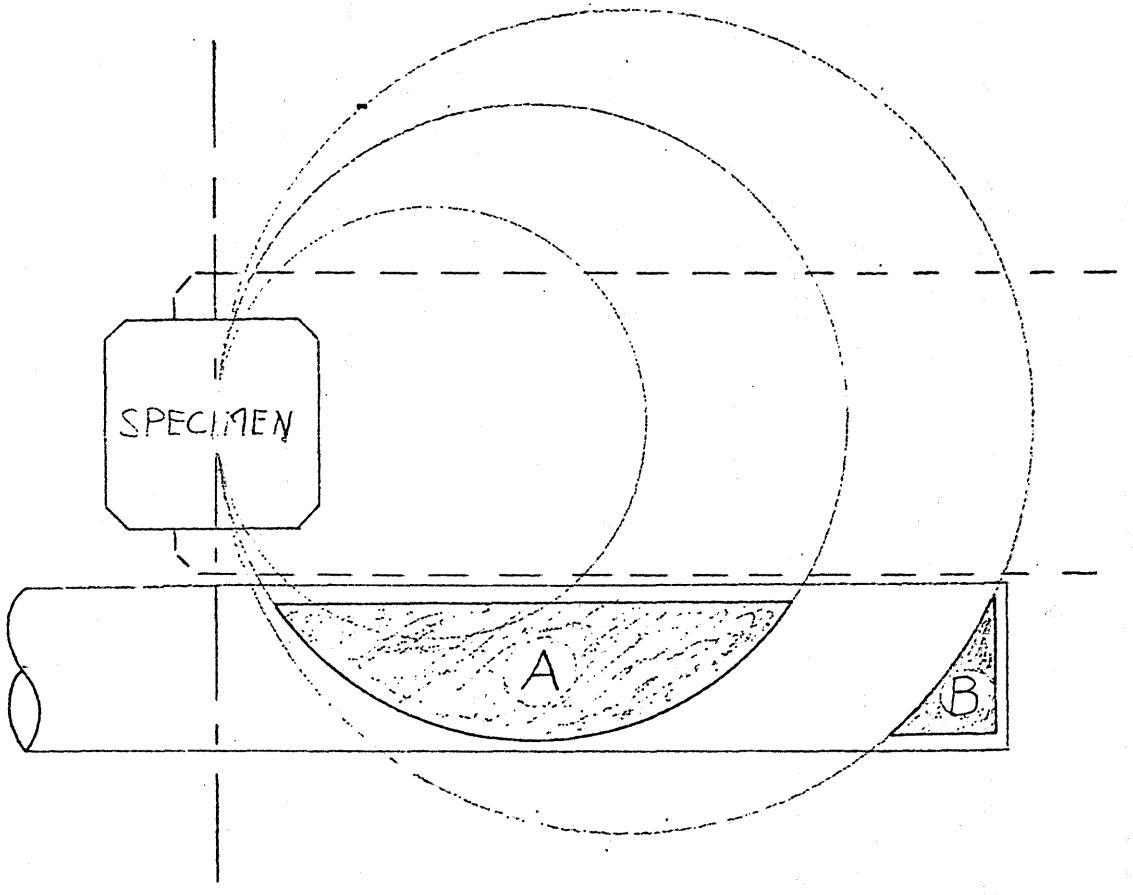

Figure 14. Curves of equal $\underline{de}_s/\underline{de}_t$.

The equations also suggest high angular rotation velocities and narrow pass bands; these factors can be considered along with others such as the described sensitivity, ease of operation, and stability of the detecting units, in the overall design of a spinner magnetometer.

COLLECTION OF SAMPLES

Although irregularly shaped samples broken from outcrops may be oriented in a variety of ways, it is often more efficient to obtain oriented samples by drilling short cores *in situ* with portable coring equipment. The regularly shaped cores can be routinely oriented with an accuracy of 2°, and sampling need not be restricted to the edges of joint blocks.

The drilling unit we employ (fig. 15) consists of the power unit from a small commercial chain saw, a special transmission (details shown in fig. 16), a commercial sintered diamond masonry coring drill, and pressure type garden insecticide spray tanks for supplying cooling water to the diamond drill. Cores 2.49 cm in diameter and from 10 to 20 cm long can be drilled from most extrusive igneous rocks with little difficulty unless the rock is highly fractured. Hard rocks that require long drilling times may be more easily drilled by fitting the coring equipment to a tripod, or similar device, that will support the weight of the unit as well as guide the core drill. Without water in the tanks, the unit weighs about 10 kilograms.

The cores are oriented with slotted tubes that can be slipped over the core before it is separated from the outcrop (fig. 15). The slotted tubes are fitted with a level so that the slot may be placed along the

Figure 15. Sample coring drill with water tank and orienting device.

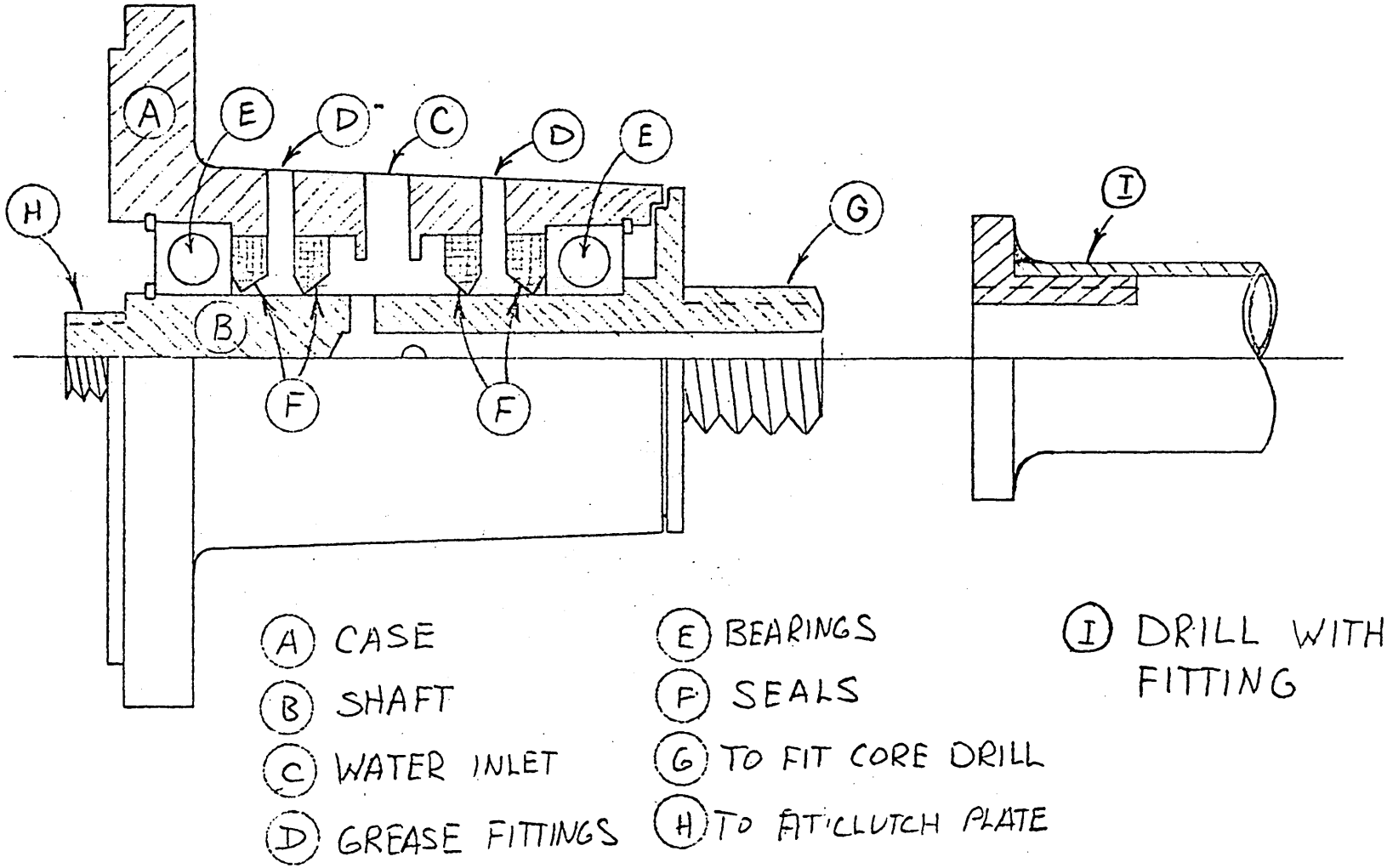

Figure 16. Mechanical details of the core drill transmission.

uppermost edge of the core (intersection of the core surface with the vertical plane passing through the core axis); they are also fitted with a magnetic compass, an inclinometer, and sighting blades for transit operation. Properly fitted, a geologist's pocket transit may also fulfill all these needs.

In our system, the core axis is the $\underline{z}$ axis, positive from the surface into the outcrop, and the $\underline{x}$ and $\underline{y}$ axes define an orthogonal system such that $\underline{y}$ always lies in the horizontal and the $+\underline{x}$ direction is always inclined above the horizontal; right-handed coordinates are used, so that the $+\underline{y}$ axis (horizontal) is directed to the right as one looks down the core axis (direction of $+z$).

A mark corresponding to the $\underline{z}$ axis is made along the upper edge of the core by slipping a brass or copper wire down the slot. The plunge of this line below (+) or above (-) the horizontal is read from the inclinometer and recorded, as is the geographic azimuth of the $+\underline{y}$ direction determined by triangulation prior to removing the core from the outcrop.

After the above operations and measurements have been repeated by normal field checking procedures, the core is removed from the outcrop and the mark along the edge is immediately made permanent by marking with a diamond scribe. At the same time, the $+\underline{y}$ direction is indicated by permanent short marks on the right side of the orientation line along the entire length of the core. In this manner each specimen later cut from the core for measurement (fig. 8) retains a complete orientation, and there is no chance of errors arising during transfer of orientation marks.

We have estimated from mechanical considerations that cores of the size described here may be routinely oriented to within $\pm 2°$ using a simple slotted tube and geologist's pocket transit. If required, accuracies of $\pm 0.5°$ can be achieved with cores of this size using sufficiently precise measuring devices and by using care in placing the orientation line on the core before it is removed from the outcrop.

An additional piece of field equipment that has proved useful in collecting samples for paleomagnetic investigation is the declination gradiometer shown in figure 17 (Doell and Cox, 1962). Two small oil-damped magnetic compasses mounted in gimbals at opposite ends of a rigid rod half a meter in length are arranged with their index marks parallel, so that the declination difference at opposite ends of the rod may easily be read as the rod is moved along an outcrop. Its purpose is to identify parts of an outcrop where lightning has struck, since the strong magnetic fields associated with lightning bolts may give igneous rocks a very strong isothermal remanent magnetization rendering them useless for paleomagnetic study (Cox, 1961; Graham, 1961). Places where this has occurred can be readily recognized by the local gradients in the magnetic field adjacent to the outcrop. Experience with lava flows has shown that measured declination gradients of less than 5° per meter, with one compass held within 10 cm of the outcrop, over an area several meters across, indicates that samples from the center of the area are sufficiently free from the effects of lightning to be suitable for paleomagnetic analysis. Declination gradients near outcrops may also be measured using a gelogist's compass.

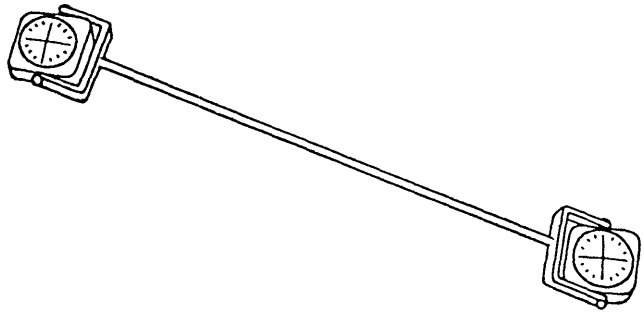

Figure 17. Declination gradiometer.

USE OF A COMPUTER TO REDUCE SPINNER-MAGNETOMETER DATA

A program for reducing spinner-magnetometer data with a digital computer is outlined below. The following conventions are used to identify the imput of this program:

$\phi_{n,m}$ ($n = x,y,z$; $m = a,b$): Phase angles between 0° and 359.9° as described in table 1. (Systematic instrumental phase angle errors as large as 90° are corrected under the assumption that the phase error for both spins about a given axis remains the same.)

$M_{n,m}$: Magnetic intensities as described in table 1.

V : Volume of the specimen in cubic centimeters.

α : In situ geographic azimuth (0° to 359.9°) of the y reference axis.

β : In situ plunge of the z axis below (+) or above (-) the horizontal.

γ : Quadrant of the horizontal projection of the z axis, according to the following convention:

Azimuth	γ
z vertical	0
0.1° to 89.9°	1
90.0° to 179.9°	2
180.0° to 269.9°	3
270.0° to 359.9°	4

The following conventions are used to identify the output of this program:

D : Declination, that is, azimuth of the horizontal component of the remanent magnetization vector restored to its in situ orientation.

I : Inclination, that is, in situ plunge of the magnetic vector below the horizontal.

M : Total magnetic moment of the specimen.

J : M/V, the magnetic intensity in emu/cc.

A : An analogue of the radius of the error triangle formed by the three great circles defined by the phase angles, as discussed below.

MM : The root mean square of the differences between the six measured magnetic intensities $M_{z,a}$, $M_{z,b}$, etc., and the ideal intensities that would be expected if the specimen acted as an ideal dipole with moment M and direction of magnetization as calculated.

To find the mean direction from the three phase-angle great circles, a comparison is first made to determine whether the three circles intersect within 0.1°. If not, an increment is added to each phase angle inversely proportional to the Nth power of the corresponding intensity M_z, M_x, or M_y, where N is retained as a parameter to be specified in the program. This process is reiterated until the common intersection is found to within 0.1°. To obtain higher precision, only the single constant in step 21 (see below) need be changed. As a measure of the lack of closure of the original error triangle, the average total increment added to the phase angles corresponding to the two strongest intensities is recorded as the quantity A.

The best value for the parameter N depends on the relationship between the accuracy of phase-angle measurements and the magnetic intensities. This, in turn, depends largely on physical considerations. If N is set equal to 0, all phase angles are weighted equally and the computer solution is essentially the center of a circle inscribed in the error triangle. This is undesirable because it gives too much weight to phase angles associated

with very weak intensities, which tend to be less reliable. On the other hand, assignment of a large number, say 5 or more, essentially eliminates from the calculation the phase angle associated with the smallest intensity, and this is undesirable where the three phase angles all have approximately the same reliability. However for very weakly magnetized specimens where only two of the three pairs of measurements are above the background noise level, a large $\underline{N}$ may be required to permit rejection of the meaningless weak measurement. On the basis of computer experiments with a wide variety of data, we have adopted a value of $\underline{N} = 2$; although no single value is adequate for all types of data, this value has proven satisfactory for almost all routine measurements made over a two-year period.

Calculation procedure

Step

1. $\phi_{n,m} \overset{?}{\leq} 180.0°$ $\qquad$ $\phi_{n,m}$: input

   yes $\quad \theta_{n,m} = \phi_{n,m}$

   no $\quad \theta_{n,m} = -(360.0° - \phi_{n,m})$

2. $(\theta_{n,a} + \theta_{n,b}) \overset{?}{<} 90.0°$

   yes $\quad \theta_n = \frac{1}{2}(\theta_{n,a} - \theta_{n,b})$

   no $\quad (\theta_{n,a} - \theta_{n,b}) \overset{?}{>} 0.0°$

   yes $\quad \theta_n = \frac{1}{2}(\theta_{n,a} - \theta_{n,b}) - 180.0°$

   no $\quad \theta_n = \frac{1}{2}(\theta_{n,a} - \theta_{n,b}) + 180.0°$

3. $M_n = \frac{1}{2}(M_{n,a} + M_{n,b})$ $\qquad$ $M_{n,m}$: input

4. $M = \left[\frac{1}{3}(M_x^2 + M_y^2 + M_z^2)\right]^{\frac{1}{2}}$ $\qquad$ M: output

5. $J = M/V$

J: output

6. $W_n = \left(1/M_n\right)^N / \left[\left(1/M_x\right)^N + \left(1/M_y\right)^N + \left(1/M_z\right)^N\right]$

N: program parameter

7. $W_z \overset{?}{\geq} W_x \overset{?}{\geq} W_y$ or $W_z \overset{?}{\geq} W_y \overset{?}{>} W_x$

yes $q = 0,\ r = 0,\ s = 1$

no $W_x \overset{?}{>} W_z \overset{?}{\geq} W_y$ or $W_x \overset{?}{\geq} W_y \overset{?}{>} W_z$

yes $q = 1,\ r = 0,\ s = 0$

no $q = 0,\ r = 1,\ s = 0$

8. $W_i = q\,W_x + r\,W_y + s\,W_z$

$W_j = s\,W_x + q\,W_y + r\,W_z$

$W_k = r\,W_x + s\,W_y + q\,W_z$

9. $\theta_i = q\,\theta_x + r\,\theta_y + s\,\theta_z$

$\theta_j = s\,\theta_x + q\,\theta_y + r\,\theta_z$

$\theta_k = r\,\theta_x + s\,\theta_y + q\,\theta_z$

10. $m_j = \cos\theta_j$

$n_j = \sin\theta_j$

$n_k = \cos\theta_k$

$\ell_k = \sin\theta_k$

11. $f = \left(1 + \ell_k^2\, n_j^2/n_k^2\right)^{-\frac{1}{2}}$

12. $\ell_{jk} = f\ \ell_k\ n_j/n_k$

$m_{jk} = f\ m_j$

$n_{jk} = f\ n_j$

13. $g = \left(\ell_{jk}^2 + m_{jk}^2\right)^{\frac{1}{2}}$

14. $g \stackrel{?}{=} 0$

yes proceed to step 35

no proceed to step 15

15. $\rho = \arccos\left(\ell_{jk}/g\right)$ $\qquad 0 \le \rho \le 180.00°$

16. $m_{jk} \stackrel{?}{\geq} 0$

yes $\theta_i' = \rho$

no $\theta_i' = -\rho$

17. $\theta_i \stackrel{?}{<} \theta_i'$

yes $\lambda = 1$

no $\lambda = 0$

18. $\theta_i'' = \theta_i - \theta_i' + \lambda\ 360.00°$

19. $\theta_i'' \stackrel{?}{\leq} 180.00°$

yes $\mu = -1$

no $\mu = 1$

20. $\theta_i''' = \frac{1}{2}(\mu + 1)\ 360.00° - \mu\ \theta_i''$

21. $g\,\theta_i''' \overset{?}{\leq} 0.07°$

yes proceed to step 35

no proceed to step 22

22. $\theta_i'^{v} = \theta_i'' \left(1 - W_i\right) + \frac{1}{2}\left(1 + \mu\right) W_i\, 360.00°$

23. $\theta_i^{v} = \theta_i'^{v} + \theta_i'$

24. $\theta_i^{v} \overset{?}{>} 180.00°$

yes $\theta_i^{v'} = \theta_i^{v} - 360.00°$

no $\theta_i^{v'} = \theta_i^{v}$

25. $\ell_k \overset{?}{=} 0$

yes $d_j = \left(n_k \cos\theta_i^{v'}\right) / \left|n_k \cos\theta_i^{v'}\right|$

no $d_j = n_k\, \ell_k / \left|n_k\, \ell_k\right|$

26. $m_j \overset{?}{=} 0$

yes $d_k = \left(n_j \sin\theta_i^{v'}\right) / \left|n_j \sin\theta_i^{v'}\right|$

no $d_k = n_j\, m_j / \left|n_j\, m_j\right|$

27. $\theta_j' = \theta_j + \theta_i'''\, \mu\, d_j\, W_j$

28. $\theta_k' = \theta_k + \theta_i'''\, \mu\, d_k\, W_k$

29. $\theta_j' \overset{?}{\leq} -180.00°$

yes $\theta_j'' = \theta_j' + 360.00°$

no $\theta_j' \overset{?}{>} 180.00°$

yes $\theta_j'' = \theta_j' - 360.00°$

no $\theta_j'' = \theta_j'$

30. $\theta_k' \overset{?}{\leq} -180.00°$

yes $\theta_k'' = \theta_k' + 360.00°$

no $\theta_k' \overset{?}{>} 180.00°$

yes $\theta_k'' = \theta_k' - 360.00°$

no $\theta_k'' = \theta_k'$

31. $A_t = \frac{1}{2}(W_j + W_k)\,\mu\,\theta_i'''$

32. Transfer A_t to storage and accumulate for all cycles through reiterative part of program.

33. Transfer to step 10 and make following substitutions:

θ_i by $\theta_i^{v'}$

θ_j by θ_j''

θ_k by θ_k''

34. Reiterate steps 10 through 33 until yes option in step 21 is reached, or until 10 reiterations have been completed. In latter case, stop calculation and print "NC." Skip steps 25 and 26 on each reiteration, retaining the values of d_j and d_k from the first cycle.

35. $\ell = s\,\ell_{jk} + r\,m_{jk} + q\,n_{jk}$

$m = q\,\ell_{jk} + s\,m_{jk} + r\,n_{jk}$

$n = r\,\ell_{jk} + q\,m_{jk} + s\,n_{jk}$

36. $A = \left| \sum_{t=1}^{T} A_t \right|$ A: output

where T is the total number of reiterations through steps 10-33.

37. $M_z' = M \left[\ell^2 + m^2 \right]^{\frac{1}{2}}$

$M_x' = M \left[m^2 + n^2 \right]^{\frac{1}{2}}$

$M_y' = M \left[n^2 + \ell^2 \right]^{\frac{1}{2}}$

38. $MM = \left(1/2.449\ M\right) \left[\left(M_z' - M_{z,a}\right)^2 + \left(M_z' - M_{z,b}\right)^2 + \left(M_x' - M_{x,a}\right)^2 + \left(M_x' - M_{x,b}\right)^2 + \left(M_y' - M_{y,a}\right)^2 + \left(M_y' - M_{y,b}\right)^2 \right]^{\frac{1}{2}}$ MM: output

39. $\gamma \stackrel{?}{=} 0$

yes $\beta \stackrel{?}{=} 90.0°$

yes $\chi = 180.0°$ skip steps 40, 41

no $\chi = 0.0°$ skip steps 40, 41

no $\alpha \stackrel{?}{<} 90.0°$

yes $\delta = 1$

no $\alpha \stackrel{?}{<} 180.00°$

yes $\delta = 2$

no $\alpha \stackrel{?}{<} 270.0°$

yes $\delta = 3$

no $\delta = 4$

40. $(\delta - \gamma) \stackrel{?}{=} 1$ or $(\delta - \gamma) \stackrel{?}{=} -3$

yes $\epsilon = 0$

no $(\delta - \gamma) \stackrel{?}{=} -1$ or $(\delta - \gamma) \stackrel{?}{=} 3$

yes $\epsilon = 1$

no stop calculation, print out "Q.E."

41. $\chi = 90.0° - \beta + \epsilon\,(2\beta + 180.0°)$

42. $\ell' = \ell \cos\chi + n \sin\chi$

$n' = -\ell \sin\chi + n \cos\chi$

43. $I = \arcsin n'$, $-90.0° \leq I \leq 90.0°$ I: output

44. $\bar{X} = m \cos\alpha + \ell' \sin\alpha$

$\bar{Y} = m \sin\alpha + \ell' \cos\alpha$

45. $D' = \arccos\left[\bar{X}/\left(\bar{X}^2 + \bar{Y}^2\right)^{\frac{1}{2}}\right]$ $0.0° \leq D' \leq 180.0°$

46. $\bar{Y} \stackrel{?}{\geq} 0.0°$ D: output

yes $D = D'$

no $D = 360.0° - D'$

REFERENCES

Bruckshaw, J. M., and Robertson, E. I., 1948, The measurement of magnetic properties of rocks: Jour. Sci. Instruments, v. 25, p. 444-446.

Cox, Allan, 1961, Anomalous remanent magnetization of basalt: U. S. Geol. Survey Bull., 1083E, p. 131-160.

Doell, R. R., and Cox, Allan, 1962, Determination of the magnetic polarity of rock samples in the field: Art. 151 in U. S. Geol. Survey Prof. Paper 450-D, p. D105-D108.

_____ 1963, The accuracy of the paleomagnetic method as evaluated from historic Hawaiian lava flows: Jour. Geophys. Research, v. 68, no. 7, p. 1997-2009.

Graham, J. W., 1949, The stability and significance of magnetism in sedimentary rocks: Jour. Geophys. Research, v. 54, no. 2, p. 131-167.

Graham, K.W.T., 1961, The re-magnetization of a surface outcrop by lightning currents: Geophys. Jour., v. 6, no. 1, p. 85-102.

Gray, T. S., ed., 1954, Applied electronics, 2d ed.: New York, John Wiley and Sons, Inc., 881 p.

Johnson, E. A., and McNish, A. G., 1938, An alternating-current apparatus for measuring small magnetic moments: Terrestrial Magnetism and Atmospheric Electricity, v. 43, p. 393-399.

Nagata, Takesi, 1961, Rock magnetism, revised ed.: Tokyo, Maruzen Co. Ltd., 350 p.